Hormonal Regulation of Osteocyte Perilacunar and Canalicular Remodeling in the Hyp Mouse Model of X-Linked Hypophosphatemia

Danielle Tokarz[1,2], **Janaina S Martins**[2,3], **Elizabeth T Petit**[3], **Charles P Lin**[1,2], **Marie B Demay**[2,3], and **Eva S Liu**[2,3,4]

[1]Advanced Microscopy Program, Center for Systems Biology and Wellman Center for Photomedicine, Massachusetts General Hospital, Boston, MA, USA

[2]Harvard Medical School, Boston, MA, USA

[3]Endocrine Unit, Massachusetts General Hospital, Boston, MA, USA

[4]Division of Endocrinology, Diabetes, and Hypertension, Brigham and Women's Hospital, Boston, MA, USA

Abstract

Osteocytes remodel their surrounding perilacunar matrix and canalicular network to maintain skeletal homeostasis. Perilacunar/canalicular remodeling is also thought to play a role in determining bone quality. X-linked hypophosphatemia (XLH) is characterized by elevated serum fibroblast growth factor 23 (FGF23) levels, resulting in hypophosphatemia and decreased production of 1,25 dihydroxyvitamin D (1,25D). In addition to rickets and osteomalacia, long bones from mice with XLH (Hyp) have impaired whole-bone biomechanical integrity accompanied by increased osteocyte apoptosis. To address whether perilacunar/canalicular remodeling is altered in Hyp mice, histomorphometric analyses of tibia and 3D intravital microscopic analyses of calvaria were performed. These studies demonstrate that Hyp mice have larger osteocyte lacunae in both the tibia and calvaria, accompanied by enhanced osteocyte mRNA and protein expression of matrix metalloproteinase 13 (MMP13) and genes classically used by osteoclasts to resorb bone, such as cathepsin K (CTSK). Hyp mice also exhibit impaired canalicular organization, with a decrease in number and branching of canaliculi extending from tibial and calvarial lacunae. To determine whether improving mineral ion and hormone homeostasis attenuates the lacunocanalicular phenotype, Hyp mice were treated with 1,25D or FGF23 blocking antibody (FGF23Ab). Both therapies were shown to decrease osteocyte lacunar size and to improve canalicular organization in tibia and calvaria. 1,25D treatment of Hyp mice normalizes osteocyte expression of MMP13 and classic osteoclast markers, while FGF23Ab

decreases expression of MMP13 and selected osteoclast markers. Taken together, these studies point to regulation of perilacunar/canalicular remodeling by physiologic stimuli including hypophosphatemia and 1,25D.

Keywords

OSTEOCYTES; BONE REMODELING; OSTEOMALACIA AND RICKETS; PTH/VIT D/ FGF23; BONE HISTOMORPHOMETRY

Introduction

Osteocytes are versatile bone cells capable of multiple functions, including sensing mechanical loading, secreting endocrine hormones that regulate mineral metabolism, and modulating bone resorption.[1–4] They reside in lacunae surrounded by mineralized matrix. [1] An extensive network of dendritic processes encased in canaliculi extends from osteocytes to allow for intracellular and extracellular communication and transport of nutrients and small molecules.[5] Studies suggest that osteocytes directly remodel the surrounding perilacunar and canalicular matrix, resorbing bone to maintain skeletal and mineral ion homeostasis.[6,7] Although PTH/PTHrP has been shown to regulate perilacunar remodeling, the roles of 1,25D and FGF23 have not been studied.[7–13]

X-linked hypophosphatemia (XLH) is characterized by a mutation in PHEX, leading to elevated serum FGF23 levels, hypophosphatemia, and suppression of vitamin D 1-alpha-hydroxyase.[3,14,15] Femurs from mice with XLH (Hyp) have dramatically impaired whole-bone biomechanical properties.[16] Improvement of mineral ion and hormone homeostasis in Hyp mice by treatment with daily 1,25 dihydroxyvitamin D (1,25D) or an anti-FGF23 blocking antibody (FGF23Ab) only partially restores bone strength and toughness, suggesting the abnormal bone quality observed XLH is in part be due to an intrinsic defect in bone cells.[16] Evaluation of the tibial cortex in Hyp mice reveals a decrease in the number of osteocytes accompanied by an increase in osteocyte apoptosis compared to wild-type (WT).[16] The increase in osteocyte apoptosis in Hyp mice may contribute to abnormalities in perilacunar bone mineral resorption and canalicular organization, which have been shown to impair biomechanical integrity.[17,18] Treatment of Hyp mice with 1,25D or FGF23Ab decreased osteocyte cell death, suggesting that abnormalities in phosphate or mineral hormone homeostasis play a role in perilacunar and canalicular remodeling.[16] Hypomineralized periosteocytic lesions also surround the osteocyte lacunae in cortical bone from patients with XLH, with these "halos" decreasing in frequency with 1,25D therapy.[19] These findings further support the possibility of abnormal osteocyte-mediated lacunocanalicular remodeling in the pathogenesis of abnormalities in Hyp bone.

Because abnormalities in perilacunar remodeling and canalicular network organization may contribute to bone quality,[17,18] studies were undertaken to examine the lacunar/canalicular network in Hyp mice. Traditional therapies of XLH do not normalize mineral ion homeostasis and can lead to complications, with oral phosphate being rapidly cleared and suppressing endogenous 1,25D[20] and treatment with combination 1,25D and phosphate leading to nephrocalcinosis.[21] Based on our previous studies demonstrating that FGF23Ab

or 1,25D administration to Hyp mice without phosphate supplementation improved histomorphometric and biomechanical outcomes,[16] we addressed the hypothesis that these therapies will also improve the Hyp lacunocanalicular phenotype. FGF23Ab treatment, in contrast to phosphate and 1,25D therapy, offers the advantage of blocking phosphate-independent actions of FGF23 along with decreasing renal phosphate excretion and transiently increasing production of 1,25D.[16]

Materials and Methods

Animal studies

Animal studies were approved by the institutional animal care committee. All mice were on a C57BL/6J background, maintained in a virus-free and parasite-free barrier facility and exposed to a 12-hour light/dark cycle. Mice were weaned on day 18 onto house chow (1% calcium, 0.6% phosphate; PMI Nutrition International, LLC, St. Louis, MO, USA; 3003219-249) and housed in up to five mice per cage. Male and female Hyp mice, randomly assigned to treatment or control groups, were subcutaneously injected daily with 1,25D (175 pg/g/day; Akorn, Inc., Lake Forest, IL) or three times per week with an FGF23 blocking antibody (FGF23Ab; 35 mcg/g; Amgen, Thousand Oaks, CA) starting on day 2.[16] Wild-type (WT) and Hyp control male and female littermates received vehicle or isotype-matched antibody (35 μg/g). Each mouse was assigned a number to permit analyses in a blinded fashion.

Histology

Tissues were fixed in 10% formalin for 24 hours, decalcified in 20% EDTA/phosphate-buffered saline (PBS) for 2 weeks, and processed for paraffin sectioning. For thionin staining,[22] sections were rehydrated, rinsed in running tap water, and immersed in 0.125% thionin (Fisher, Hampton, NH) for 15 min. Following a rinse in tap water, the sections were immersed in 1.3% picric acid (Sigma, St Louis, MO) and dehydrated in 100% alcohol. To analyze the canalicular structure, the number of dendritic processes per osteocyte, connections between pairs of adjacent osteocytes (connectivity), and bifurcating canaliculi extending from each lacuna (branching) were manually quantitated. Ten osteocytes (for number of dendritic processes/osteocyte and branching) and five osteocyte pairs (for connectivity) from four regions of the cortical bone midway between the periosteal and endosteal surfaces at the tibial mid-shaft contralateral to the tibia-fibula junction visualized at magnification ×40 were analyzed from each mouse. The analysis was performed on individual lacunae or pairs of lacunae with canaliculi extending around the entire circumference of the lacunae.

For Picrosirius Red staining, sections were rehydrated, stained with hematoxylin, and then immersed in Picrosirius Red solution (1% Sirius Red (Sigma) in 1.3% picric acid) for 1 hour. Sections were washed in acidified water and dehydrated in 100% alcohol. Collagen alignment was visualized using polarized light microscopy.

Histomorphometry

Periosteocytic lacunar area (Lac.Ar) in the lateral tibial cortex, 5 mm above the tibia-fibula junction, was quantitated on paraffin sections at a magnification of ×40 using an Osteomeasure image analyzer (Osteometrics, Atlanta, GA, USA). Because Hyp cortices have decreased osteocyte number relative to WT,[16] Lac.Ar was normalized to osteocyte number.

Intravital microscopy: third harmonic generation imaging

Third harmonic generation (THG) microscopy is a form of nonlinear microscopy in which simultaneous arrival of three photons at the sample results in one scattered photon at exactly 1/3 of the wavelength, or three times the energy. In this case a femtosecond (fs) fiber laser at 1550 nm was used and the signal detected at 515 nm. The signal is generated predominantly at interfaces between different materials, such as between bone and the interstitial fluid, without the need for labeling with a fluorescent dye as in conventional multiphoton microscopy. The nonlinear process automatically gives rise to optical sectioning, which can be used to construct 3D images.

Mice were anesthetized with isoflurane and placed in a custom heated mouse holder. An incision was made in the scalp to expose the periosteum and the calvarial bone. The dissected area was hydrated with PBS and covered with a microscope cover glass. Calvarial osteocytes were imaged with an in-house three-photon excitation microscope.[23] Images were obtained of four areas of the calvaria bordering the sagittal and coronal sutures in the frontal and parietal bones. Briefly, a 5-MHz repetition rate, 370-fs duration pulses, and 1550-nm wavelength laser (FLCPA-01CCNL41; Calmar, Palo Alto, CA) was coupled to a polarization maintaining large mode area single-mode photonic crystal fiber (LMA40; NKT Photonics, Birkerod, Denmark) for pulse compression. The compressed pulse was coupled to a laser scanning microscope that consisted of a polygonal laser scanner (DT-36-290-025; Lincoln Laser, Phoenix, AZ) and a galvanometric scanning mirror (6240H; Cambridge Technology, Cambridge, MA) achieving 15 frames per second with 500×500 pixels. An oil immersion objective lens (1.05 NA, UPLSAPO 30×SIR; Olympus, Waltham, MA) with mineral oil (Sigma Aldrich) was used for excitation and collection. THG signals were separated with dichroic mirrors from the laser (DMLP950R; Thorlabs Inc., Newton, NJ), filtered (65–153; Edmund Optics, Barrington, NJ) and collected using a photomultiplier tube (R7600U-300; Hamamatsu, Hammatsu City, Japan). The THG channel was digitized with 8 bits at the laser repetition rate using the laser sync output as a pixel clock with a frame grabber card (Snapper-PCI-8/24; Active Silicon, Severna Park, MD).

ImageJ 1.50i (NIH) was used to analyze 2D lacunar surface area, width, and height. Lacunar width corresponds with the short elliptical axis length, whereas lacunar height refers to the long elliptical axis length. The lacunar area per osteocyte was measured by examining optical sections taken with 1-μm increments and selecting the slice that corresponded to the center of the lacuna (the slice in which the lacunar area appeared the largest). A small region containing the center of the lacuna was selected, the region was manually thresholded so that only signal from the lacuna was present, and the area as well as the % area functions were used to calculate the lacunar area.

3D analysis of osteocytes was performed in ImageJ and Imaris 7.4.2 (Oxford Instruments, Abingdon, UK). The number of osteocytes in a volume of 100 μm × 100 μm × 10 μm was manually counted in ImageJ by selecting this volume from optical sections. In Imaris, the lacunar volume and surface area of individual lacuna were calculated by manual thresholding of the signal intensity from the lacunae and allowing the software to calculate these properties. The number of canaliculi per osteocyte was determined by imaging the calvaria with an image size of 244 μm × 147 μm. The images were manually thresholded in Imaris, the FilamentTracer function was used to trace the canaliculi, and then the number of canaliculi was manually counted. For all 2D and 3D THG analyses, 20 osteocytes from four regions in the calvaria bordering the coronal and sagittal sutures in the frontal and parietal bones were analyzed from each mouse.

Osteocyte gene expression

Osteocyte RNA was isolated from mouse bone, using a modification of the protocol described in Qing and colleagues.[7] Femurs were dissected from day 30 (d30) mice, after the epiphyses were cut off and the diaphyses were subjected to centrifugation and flushing with PBS to remove the bone marrow. The remaining femoral cortical shafts were sequentially digested to remove osteoblasts, osteoclasts, periosteal cells, and other adherent cells. Femur cortices were subjected to three sequential digestions in 0.2% type 1 collagenase (Worthington, Lakewood, NJ)/0.05% trypsin (Thermo Fisher Scientific) in α-MEM media/25 mM HEPES/0.1% BSA. Following a PBS wash, they were incubated with 0.53 mM EDTA/0.05% trypsin in PBS/0.1% BSA, after which they were incubated with 0.2% type 1 collagenase/0.05% trypsin. Digests were shaken at 900 rpm for 30 min at 37°C in a ThermoMixer R (Eppendorf). Digested femur cortices were homogenized in Trizol (Thermo Fisher Scientific). Total RNA was isolated as described[16] and reverse transcribed with SuperScript II (Roche). Quantitative real time-PCR was performed using the QuantiTect SYBR Green RT-PCR kit (Qiagen, Hilden, Germany) on an Opticon DNA engine (MJ Research, Waltham, MA). Gene expression was normalized to that of WT for each sample, using the methods of Livak and Schmittgen.[24]

Immunohistochemistry

Paraffin sections were blocked with 10% heat inactivated fetal bovine serum (FBS). After incubation with anti-cathepsin K antibody (1:200; Abcam, Cambridge, MA; ab19027), signal detection was performed using biotinylated goat-anti rabbit secondary antibody (Vector, Burlingame, CA) followed by incubation with avidin-biotin complex (Vecta Stain; PK-6100). For matrix metalloproteinase 13 (MMP13) immunohistochemistry, following antigen retrieval with proteinase K at 37°C sections were incubated with anti-MMP13 antibody (1:200; Abcam; ab39012). Signal was detected using goat anti-rabbit HRP (Santa Cruz or Sigma, Dallas, TX).

Statistical analysis

All data shown are reported as mean ± standard deviation (SD). One-way ANOVA followed by Fisher's least significant difference (LSD) test was used to analyze significance between all control and treatment groups. Significance was defined as $p < 0.05$.

Results

Hyp tibias and calvariae have increased osteocyte lacunar area and abnormal canalicular organization

The tibial cortices of Hyp mice exhibit an increase in osteocyte apoptosis compared to WT. [16] Because osteocytes remodel their perilacunar matrix and their canalicular network is needed for cell-cell communication, [17] the increased osteocyte cell death in Hyp mice may be associated with alterations in osteocyte-mediated perilacunar and canalicular remodeling. To evaluate the osteocyte lacunocanalicular network, the tibial cortices of d75 WT and Hyp mice were examined. Hematoxylin and eosin (H&E) staining shows that the Hyp tibial osteocyte lacunae are larger than WT (Fig. 1*A*). Histomorphometric quantification of the osteocyte Lac.Ar was normalized to osteocyte number because of the significant decrease in osteocyte number in Hyp mice relative to WT.[16] The Lac.Ar/osteocyte value was found to be significantly larger in Hyp mice than in WT mice (Fig. 1*A*), suggesting increased osteocyte-mediated perilacunar matrix remodeling. Because the canaliculi are necessary for communication and transport of nutrients between cells,[5] the increased osteocyte apoptosis observed in Hyp tibias suggests that the canalicular organization of Hyp cortices could be altered. Thionin staining of the canalicular network revealed abundant canaliculi in WT mice, with dendritic processes extending from each osteocyte to form an extensive branched intercellular network. In contrast, the canaliculi of Hyp mice are sparse and short (Fig. 1*B*). Compared to WT, Hyp osteocytes have decreased number of canaliculi, decreased canalicular branching and dramatically decreased canalicular connectivity (Fig. 1*B*).

To analyze the 3D properties of the osteocyte lacunae, intravital THG microscopy of calvarial osteocyte lacunae was performed. Similar to the long bone phenotype, Hyp calvarial osteocyte lacunae are larger and the canaliculi are sparser than WT (Fig. 2*A*). The density of lacunae, lacunar volume, and 3D lacunar surface area in Hyp calvaria are significantly greater than that of WT (Fig. 2*B*). Additionally, Hyp osteocytes have a significant decrease in canalicular density and canalicular branching compared with WT (Fig. 2*C*).

Osteocyte-enriched bone from Hyp mice has increased expression of markers of perilacunar remodeling

Osteocytes express genes characteristic of osteoclast-mediated bone resorption.[7] The expression of these genes is enhanced during the remodeling of periosteocytic lacunar matrix.[7] Because of the increased size of Hyp osteocyte lacunae, RNA was isolated from osteocyte enriched femoral bone to determine whether Hyp osteocytes have increased expression of markers of perilacunar remodeling. Consistent with the XLH phenotype, expression of FGF23 and matrix extracellular phosphoglycoprotein (MEPE)[25] by Hyp osteocytes is significantly increased relative to WT. The expression of dentin matrix acidic phosphoprotein 1 (DMP1) is not different between WT and Hyp, confirming analogous populations of osteocytes in the osteocyte enriched WT and Hyp bone (Fig. 3*A*). Analyses of classic osteoclast genes demonstrate a significant increase in the expression of cathepsin K (CTSK) and tartrate-resistant acid phosphatase (TRAP) in Hyp osteocytes (Fig. 3*B*). Expression of genes traditionally expressed by osteoclasts to acidify the extracellular

environment during bone resorption including chloride channel 7 (CLCN7), ATPase H+ transporting lysosomal V0 subunit (ATP6V0D2), and Na+/H+ exchanger domain containing 2 (NHEDC2) are also enhanced in Hyp osteocytes.[26–28] Osteocyte expression of carbonic anhydrase 2 (CAR2), which regulates extracellular acidification,[27] and E11/gp38, which regulates dendritic elongation,[29] are not altered in Hyp mice (Fig. 3*B*). Immunohistochemistry confirmed an increase in cathepsin K protein in the osteocytes of d14 and d30 in Hyp calvariae and tibias (Fig. 3*C*).

MMP13 is required to maintain canalicular organization and enhances remodeling of perilacunar matrix in cortical bone.[18] Its expression is increased in osteocytes during lactation-induced perilacunar mineral resorption.[11] Similarly, Hyp osteocytes express significantly higher MMP13 mRNA levels relative to WT, which corresponds to the increased MMP13 immunoreactivity observed in d14 and d30 calvarial and tibial osteocytes (Fig. 3*B, D*). These results suggest that enhanced expression of markers of perilacunar and canalicular remodeling by Hyp osteocytes mediates the increased perilacunar bone resorption observed.

Treatment of Hyp mice with 1,25D or FGF23Ab decreases lacunar size and improves canalicular organization

To determine the relative roles of decreased 1,25D production or increased FGF23 expression in the increased perilacunar remodeling observed in the Hyp model of XLH, Hyp mice were treated daily with 1,25D or three times/week with FGF23Ab. As previously reported, daily 1,25D or FGF23Ab treatment maintains normocalcemia while similarly improving serum phosphate and normalizing serum PTH levels.[16] By day 75 (73 days of therapy), both 1,25D and FGF23Ab treatment of Hyp mice normalized lacunar area and decreased the hypomineralized halos surrounding osteocytes (Fig. 4*A*). Thionin staining demonstrates partial restoration of canalicular network organization by both treatments (Fig. 4*B*). Both therapies also increase the number of canaliculi extending from each lacunae and improve canalicular connectivity and branching (Fig. 4*B*). Because impaired collagen cleavage leads to abnormal canalicular structure, Picrosirius Red stain was performed to visualize collagen alignment, with no alterations observed in either the untreated Hyp or treated Hyp mice (Fig. 4*C*).

THG imaging analyses of Hyp mice treated from day 2 to 30 show that 1,25D or FGF23Ab therapy significantly attenuates the increase in the 2D and 3D surface areas of calvarial osteocyte lacunae in Hyp mice (Fig. 5*A–C*). Neither lacunar density nor lacunar volume are altered by daily 1,25D treatment, but FGF23Ab improves these parameters (Fig. 5*C*). Although lacunae of untreated Hyp mice are significantly wider and taller than those of WT mice, 1,25D and FGF23Ab both decrease the width, but not the height, of the osteocyte lacunae (Fig. 5*B*). Both therapies increase the density of branched canaliculi relative to Hyp control, whereas FGF23Ab treatment also improves the total canalicular density (Fig. 5*D*).

Daily 1,25D treatment of Hyp mice suppresses markers of perilacunar remodeling more than FGF23Ab treatment

Because improving serum phosphate or 1,25D levels or blocking FGF23 action attenuates the increased perilacunar remodeling and partially restores the canalicular organization in Hyp mice, studies were undertaken to determine the effects of these treatments on the expression of markers of perilacunar and canalicular remodeling in osteocyte-enriched Hyp bone. RT-qPCR analyses demonstrate that both daily 1,25D and FGF23Ab therapies significantly increase the expression of FGF23 and MEPE mRNA in Hyp osteocytes while the expression of DMP1 is not altered by either treatment (Fig. 6*A*). 1,25D treatment of Hyp mice normalizes the mRNA expression of perilacunar/canalicular remodeling markers CTSK, TRAP, MMP13, ATP6V0D2, and NHEDC2. 1,25D also suppresses expression of CLCN7 to below that observed in WT and increases expression of E11/gp38 relative to WT (Fig. 6*B*). FGF23Ab treatment of Hyp mice significantly decreases osteocyte gene expression of MMP13, CLCN7, ATP6V0D2, and NHEDC2, but does not alter expression of CTSK, TRAP, or E11/gp38 (Fig. 6*B*). Corresponding to these mRNA expression analyses, daily 1,25D treatment normalizes cathepsin K and MMP13 immunoreactivity in Hyp calvarial and tibial osteocytes (Fig. 6*C, D*). Treatment of Hyp mice with FGF23Ab does not uniformly decrease cathepsin K immunoreactivity in calvarial and tibial osteocytes, but does normalize that of MMP13 (Fig. 6*C, D*).

Discussion

XLH is characterized by inactivating mutations of the PHEX gene, which is expressed predominantly in osteocytes.[14,30,31] The current treatment for XLH, a combination of phosphate and 1,25D supplementation, does not normalize skeletal mineralization in affected individuals.[21,32,33] Similarly, Hyp mice treated with phosphate, 1,25D, or therapies that target FGF23 action exhibit persistent abnormalities in skeletal mineralization, microarchitecture, and biomechanics.[16,34] Long bones or osteoblasts isolated from Hyp mice transplanted into WT mice continue to exhibit impaired mineralization, suggesting an intrinsic defect in Hyp osteoblasts or osteocytes.[35–37] Therefore, the observation that improving mineral ion and hormone homeostasis does not prevent skeletal defects in Hyp mice supports the previous finding of intrinsic abnormalities in osteoblast and/or osteocyte function.

We have previously shown an increase in osteocyte apoptosis accompanied by a decrease in osteocyte number in the cortical bone of Hyp mice.[16] Current studies demonstrate that Hyp cortical bone exhibits fewer canaliculi as well as impaired canalicular branching. The similar canalicular phenotype in the weight-bearing tibia and the non–weight-bearing calvaria suggest that mechanical loading does not underlie the abnormal canalicular network observed in Hyp mice. Treatment of Hyp mice with either 1,25D or FGF23Ab only partially restores the canalicular structure, suggesting that intrinsic abnormalities of Hyp osteocytes including increased osteocyte death contribute to the lacunocanalicular abnormalities observed in Hyp mice. Alternatively, because the osteocyte canalicular network is necessary for cell-cell communication and transport of nutrients, proteins, and small molecules, the increase in osteocyte apoptosis in Hyp mice may be secondary to abnormal canalicular

organization.[17] In support of this latter hypothesis, an increase in osteocyte cell death due to B-cell lymphoma (Bcl2) overexpression is accompanied by a decrease in the number of dendritic processes extending from osteocytes.[38] Mice lacking metalloproteinase 2 (MMP2) or the von Hippel-Lindau gene (Vhl) also exhibit a decrease in number of canaliculi and canalicular connectivity associated with an increase in osteocyte apoptosis. [39,40] These mouse models support the important role of the osteocyte canalicular network on osteocyte viability.

Studies in mice with ablation of MMP13, a bone matrix protein that cleaves type I collagen and maintains bone quality, revealed that MMP13 is required for the formation of a normal osteocyte canalicular network as well as the increased perilacunar remodeling observed during lactation.[18] Degradation of the extracellular matrix by proteins like MMP13 is thought to be necessary for canalicular network formation.[18] In support of this, the canalicular structure is impaired in *Col1a1r/r* mice, which express a type 1 collagen mutant that cannot be cleaved by MMPs.[39] Similarly, bones from mice lacking Membrane type 1-matrix metalloproteinase 1 (MT1-MMP) or metalloproteinase 2 (MMP2) also have sparse and ill formed canaliculi.[39,41] The current studies demonstrate that despite the enhanced expression of MMP13 in Hyp osteocytes, their canalicular network organization is still markedly abnormal. Collagen crosslinking in Hyp mice has been reported to be unaltered[42] and our studies similarly demonstrate no changes in collagen structure in control and treated Hyp cortical bone. Therefore, factors other than abnormal collagen organization and MMP cleavage likely contribute to the defect in canalicular structure observed. Notably, DMP1 mutations in humans lead to autosomal recessive hypophosphatemic rickets, which is also accompanied by periosteocytic osteoid "halos" and sparse canaliculi.[43] Humans with vitamin D deficiency also exhibit poor canalicular connectivity.[44] These studies suggest that the impaired skeletal mineralization characteristic of Hyp mice contributes to the poor canalicular organization observed. The improvement in canalicular organization seen with 1,25D or FGF23Ab treatment of Hyp mice could be due to improved skeletal mineralization, [16] or direct effects of phosphate or 1,25D on canaliculi formation.

During lactation, an increase in osteocyte lacunar size is observed. Qing and colleagues[7] demonstrated that an increase in perilacunar mineral resorption during lactation corresponds with enhanced expression of MMP13 and genes used by osteoclasts to regulate bone resorption, such as CTSK and TRAP. Similar to these studies, the current data demonstrate that the enlarged osteocyte lacunae and periosteocytic hypomineralized halos in Hyp mice are also associated with increased expression of these genes. The decrease in size of the periosteocytic lacunae and hypomineralized halos with 1,25D or FGF23Ab treatment of Hyp mice is accompanied by decreased expression of MMP13. In vitro expression of MMP13 in preosteoblasts or chondrocytes is enhanced by 1,25D[45,46]; therefore, the paradoxical suppression of MMP13 expression in osteocytes of 1,25D-treated or FGF23Ab-treated Hyp mice suggests that improvement in mineral ion homeostasis and/or suppression of PTH[47] underlies this decrease in MMP13.

Our previous studies demonstrate that Hyp cortical bone have decreased mRNA expression of genes that regulate skeletal mineralization, including genes that promote mineralization (ANK and PHOSPHO1) as well as genes that inhibit mineralization (matrix gla protein

[MGP]) and bone formation (sclerostin [SOST]).[16] The current studies confirm that Hyp osteocytes have an increased expression of the mineralization inhibitor MEPE. Daily 1,25D therapy dramatically increases the expression of all these genes, while FGF23Ab increases expression of some genes including ANK, MEPE, and SOST.[16] It is possible that the improvement in mineralization seen with 1,25D or FGF23Ab therapy,[16] leads to decreased lacunar size in Hyp mice. It has been shown that 1,25D stimulates SOST expression[48] and that sclerostin stimulates perilacunar matrix resorption[49]; therefore, it is paradoxical that the increased SOST expression in treated Hyp mice is associated with improvement in lacunar size.

Enlargement of the periosteocytic lacunae is seen in rats chronically treated with PTH[50] and in patients with primary hyperparathyroidism or chronic renal disease induced secondary hyperparathyroidism.[12,13] Enhanced PTH/PTHrP action associated with the increased calcium demand during lactation in mice, also results in larger lacunar size. Of note, tibial cortical osteocytes of mice injected with PTHrP exhibit an increase in TRAP activity.[7] These findings suggest that PTH/PTHrP action enhances perilacunar remodeling to enable the release of calcium from the skeleton.[8] However, whether perilacunar remodeling is regulated by other mineral ion–regulating hormones such as 1,25D or FGF23 is not known. Because 1,25D or FGF23Ab treatment of Hyp mice increases serum phosphate and 1,25D while normalizing PTH,[16] the improvement in osteocyte lacunar parameters with these therapies could be due to the normalization of serum PTH, increase in serum phosphate or direct effects of these treatments on the osteocyte.

The change in osteocyte lacunar size in Hyp mice, in the setting of increased osteocyte expression of osteoclast genes, supports the finding that osteoclast gene expression by osteocytes mediates perilacunar remodeling.[7] 1,25D treatment of Hyp mice decreases osteocyte lacunar size and osteocyte expression of osteoclast genes. The current studies suggest that 1,25D has a direct effect on osteocyte function, regulating perilacunar remodeling. Although FGF23Ab therapy suppresses acidification markers, is not as effective as 1,25D in reversing abnormal expression of other perilacunar remodeling markers. However, because it is able to similarly improve lacunar size in Hyp mice, this suggests that suppressing the osteocytes' ability to acidify their extracellular environment is sufficient to inhibit perilacunar matrix resorption. Because both 1,25D and FGF23Ab therapies improve the perilacunar/canalicular phenotype in Hyp mice, despite the dramatic increase in FGF23 seen with 1,25D, it is unlikely that FGF23 regulates osteocyte-mediated canaliculi formation and perilacunar mineral release.

Acknowledgments

References

1. Bonewald LF. The amazing osteocyte. J Bone Miner Res. 2011; 26(2):229–38. [PubMed: 21254230]
2. Nakashima T, Hayashi M, Fukunaga T, et al. Evidence for osteocyte regulation of bone homeostasis through RANKL expression. Nat Med. 2011; 17(10):1231–4. [PubMed: 21909105]

3. Liu S, Zhou J, Tang W, Jiang X, Rowe DW, Quarles LD. Pathogenic role of Fgf23 in Hyp mice. Am J Physiol Endocrinol Metab. 2006; 291(1):E38–49. [PubMed: 16449303]

4. Gluhak-Heinrich J, Ye L, Bonewald LF, et al. Mechanical loading stimulates dentin matrix protein 1 (DMP1) expression in osteocytes in vivo. J Bone Miner Res. 2003; 18(5):807–17. [PubMed: 12733719]

5. Knothe Tate ML, Adamson JR, Tami AE, Bauer TW. The osteocyte. Int J Biochem Cell Biol. 2004; 36(1):1–8. [PubMed: 14592527]

6. Baylink DJ, Wergedal JE. Bone formation by osteocytes. Am J Physiol. 1971; 221(3):669–78. [PubMed: 5570322]

7. Qing H, Ardeshirpour L, Pajevic PD, et al. Demonstration of osteocytic perilacunar/canalicular remodeling in mice during lactation. J Bone Miner Res. 2012; 27(5):1018–29. [PubMed: 22308018]

8. Wysolmerski JJ. Osteocytic osteolysis: time for a second look? Bonekey Rep. 2012; 1:229. [PubMed: 24363929]

9. Belanger LF. Osteocytic osteolysis. Calcif Tissue Res. 1969; 4(1):1–12. [PubMed: 4310125]

10. Belanger LF, Robichon J. Parathormone-induced osteolysis in dogs. A microradiographic and alpharadiographic survey. J Bone Joint Surg Am. 1964; 46:1008–12. [PubMed: 14192496]

11. Qing H, Bonewald LF. Osteocyte remodeling of the perilacunar and pericanalicular matrix. Int J Oral Sci. 2009; 1(2):59–65. [PubMed: 20687297]

12. Mosekilde L, Melsen F. A tetracycline-based histomorphometric evaluation of bone resorption and bone turnover in hyperthyroidism and hyperparathyroidism. Acta Med Scand. 1978; 204(1–2):97–102. [PubMed: 685737]

13. Bonucci E, Gherardi G. Osteocyte ultrastructure in renal osteodystrophy. Virchows Arch A Pathol Anat Histol. 1977; 373(3):213–31. [PubMed: 140505]

14. Holm IA, Huang X, Kunkel LM. Mutational analysis of the PEX gene in patients with X-linked hypophosphatemic rickets. Am J Hum Genet. 1997; 60(4):790–7. [PubMed: 9106524]

15. Jonsson KB, Zahradnik R, Larsson T, et al. Fibroblast growth factor 23 in oncogenic osteomalacia and X-linked hypophosphatemia. N Engl J Med. 2003; 348(17):1656–63. [PubMed: 12711740]

16. Liu ES, Martins JS, Raimann A, et al. 1,25-Dihydroxyvitamin D alone improves skeletal growth, microarchitecture and strength in a murine model of XLH, despite enhanced FGF23 expression. J Bone Miner Res. 2016; 31(5):929–39. [PubMed: 26751835]

17. Bonewald LF. Generation and function of osteocyte dendritic processes. J Musculoskelet Neuronal Interact. 2005; 5(4):321–4. [PubMed: 16340122]

18. Tang SY, Herber RP, Ho SP, Alliston T. Matrix metalloproteinase-13 is required for osteocytic perilacunar remodeling and maintains bone fracture resistance. J Bone Miner Res. 2012; 27(9):1936–50. [PubMed: 22549931]

19. Marie PJ, Glorieux FH. Relation between hypomineralized periosteocytic lesions and bone mineralization in vitamin D-resistant rickets. Calcif Tissue Int. 1983; 35(4–5):443–8. [PubMed: 6311372]

20. Meyer RA Jr, Meyer MH, Morgan PL. Effects of altered diet on serum levels of 1,25-dihydroxyvitamin D and parathyroid hormone in X-linked hypophosphatemic (Hyp and Gy) mice. Bone. 1996; 18(1):23–8. [PubMed: 8717533]

21. Harrell RM, Lyles KW, Harrelson JM, Friedman NE, Drezner MK. Healing of bone disease in X-linked hypophosphatemic rickets/osteomalacia. Induction and maintenance with phosphorus and calcitriol. J Clin Invest. 1985; 75(6):1858–68. [PubMed: 3839245]

22. Allison RT. Picro-thionin (Schmorl) staining of bone and other hard tissues. Br J Biomed Sci. 1995; 52(2):162–4. [PubMed: 8520253]

23. Tokarz D, Cisek R, Wein MN, et al. Intravital imaging of osteocytes in mouse cavaria using third harmonic generation microscopy. PLoS One. 2017; 12(10):e0186846. [PubMed: 29065178]

24. Livak KJ, Schmittgen TD. Analysis of relative gene expression data using real-time quantitative PCR and the 2(−Delta Delta C(T)) method. Methods. 2001; 25(4):402–8. [PubMed: 11846609]

25. Addison WN, Nakano Y, Loisel T, Crine P, McKee MD. MEPE-ASARM peptides control extracellular matrix mineralization by binding to hydroxyapatite: an inhibition regulated by PHEX cleavage of ASARM. J Bone Miner Res. 2008; 23(10):1638–49. [PubMed: 18597632]

26. Wu H, Xu G, Li YP. Atp6v0d2 is an essential component of the osteoclast-specific proton pump that mediates extracellular acidification in bone resorption. J Bone Miner Res. 2009; 24(5):871–85. [PubMed: 19113919]

27. Rousselle AV, Heymann D. Osteoclastic acidification pathways during bone resorption. Bone. 2002; 30(4):533–40. [PubMed: 11934642]

28. Ha BG, Hong JM, Park JY, et al. Proteomic profile of osteoclast membrane proteins: identification of Na+/H+ exchanger domain containing 2 and its role in osteoclast fusion. Proteomics. 2008; 8(13):2625–39. [PubMed: 18600791]

29. Zhang K, Barragan-Adjemian C, Ye L, et al. E11/gp38 selective expression in osteocytes: regulation by mechanical strain and role in dendrite elongation. Mol Cell Biol. 2006; 26(12):4539–52. [PubMed: 16738320]

30. Yuan B, Takaiwa M, Clemens TL, et al. Aberrant Phex function in osteoblasts and osteocytes alone underlies murine X-linked hypophosphatemia. J Clin Invest. 2008; 118(2):722–34. [PubMed: 18172553]

31. Martin A, Liu S, David V, et al. Bone proteins PHEX and DMP1 regulate fibroblastic growth factor Fgf23 expression in osteocytes through a common pathway involving FGF receptor (FGFR) signaling. FASEB J. 2011; 25(8):2551–62. [PubMed: 21507898]

32. Chesney RW, Mazess RB, Rose P, Hamstra AJ, DeLuca HF, Breed AL. Long-term influence of calcitriol (1,25-dihydroxyvitamin D) and supplemental phosphate in X-linked hypophosphatemic rickets. Pediatrics. 1983; 71(4):559–67. [PubMed: 6300745]

33. Marie PJ, Travers R, Glorieux FH. Bone response to phosphate and vitamin D metabolites in the hypophosphatemic male mouse. Calcif Tissue Int. 1982; 34(2):158–64. [PubMed: 6282410]

34. Marie PJ, Travers R, Glorieux FH. Healing of rickets with phosphate supplementation in the hypophosphatemic male mouse. J Clin Invest. 1981; 67(3):911–4. [PubMed: 6259210]

35. Ecarot B, Glorieux FH, Desbarats M, Travers R, Labelle L. Defective bone formation by Hyp mouse bone cells transplanted into normal mice: evidence in favor of an intrinsic osteoblast defect. J Bone Miner Res. 1992; 7(2):215–20. [PubMed: 1315116]

36. Ecarot-Charrier B, Glorieux FH, Travers R, Desbarats M, Bouchard F, Hinek A. Defective bone formation by transplanted Hyp mouse bone cells into normal mice. Endocrinology. 1988; 123(2):768–73. [PubMed: 3293983]

37. Liu S, Tang W, Zhou J, Vierthaler L, Quarles LD. Distinct roles for intrinsic osteocyte abnormalities and systemic factors in regulation of FGF23 and bone mineralization in Hyp mice. Am J Physiol Endocrinol Metab. 2007; 293(6):E1636–44. [PubMed: 17848631]

38. Moriishi T, Maruyama Z, Fukuyama R, et al. Overexpression of Bcl2 in osteoblasts inhibits osteoblast differentiation and induces osteocyte apoptosis. PLoS One. 2011; 6(11):e27487. [PubMed: 22114675]

39. Inoue K, Mikuni-Takagaki Y, Oikawa K, et al. A crucial role for matrix metalloproteinase 2 in osteocytic canalicular formation and bone metabolism. J Biol Chem. 2006; 281(44):33814–24. [PubMed: 16959767]

40. Zuo GL, Zhang LF, Qi J, et al. Activation of HIFa pathway in mature osteoblasts disrupts the integrity of the osteocyte/canalicular network. PLoS One. 2015; 10(3):e0121266. [PubMed: 25806791]

41. Holmbeck K, Bianco P, Pidoux I, et al. The metalloproteinase MT1-MMP is required for normal development and maintenance of osteocyte processes in bone. J Cell Sci. 2005; 118(Pt 1):147–56. [PubMed: 15601659]

42. van der Rest M, de Miguel E, Glorieux FH. The collagen crosslinking in the hypophosphatemic male mouse. Calcif Tissue Int. 1981; 33(1):77–9. [PubMed: 6780158]

43. Feng JQ, Ward LM, Liu S, et al. Loss of DMP1 causes rickets and osteomalacia and identifies a role for osteocytes in mineral metabolism. Nat Genet. 2006; 38(11):1310–5. [PubMed: 17033621]

44. Rolvien T, Krause M, Jeschke A, et al. Vitamin D regulates osteocyte survival and perilacunar remodeling in human and murine bone. Bone. 2017; 103:78–87. [PubMed: 28666969]

45. Chen D, Li Y, Dai X, et al. 1,25-Dihydroxyvitamin D3 activates MMP13 gene expression in chondrocytes through p38 MARK pathway. Int J Biol Sci. 2013; 9(6):649–55. [PubMed: 23847446]

46. Meyer MB, Benkusky NA, Pike JW. Selective distal enhancer control of the Mmp13 gene identified through clustered regularly interspaced short palindromic repeat (CRISPR) genomic deletions. J Biol Chem. 2015; 290(17):11093–107. [PubMed: 25773540]

47. Uchida M, Yamato H, Nagai Y, et al. Parathyroid hormone increases the expression level of matrix metalloproteinase-13 in vivo. J Bone Miner Metab. 2001; 19(4):207–12. [PubMed: 11448012]

48. Wijenayaka AR, Yang D, Prideaux M, et al. 1alpha,25-dihydroxyvitamin D3 stimulates human SOST gene expression and sclerostin secretion. Mol Cell Endocrinol. 2015; 413:157–67. [PubMed: 26112182]

49. Kogawa M, Wijenayaka AR, Ormsby RT, et al. Sclerostin regulates release of bone mineral by osteocytes by induction of carbonic anhydrase 2. J Bone Miner Res. 2013; 28(12):2436–48. [PubMed: 23737439]

50. Tazawa K, Hoshi K, Kawamoto S, Tanaka M, Ejiri S, Ozawa H. Osteocytic osteolysis observed in rats to which parathyroid hormone was continuously administered. J Bone Miner Metab. 2004; 22(6):524–9. [PubMed: 15490261]
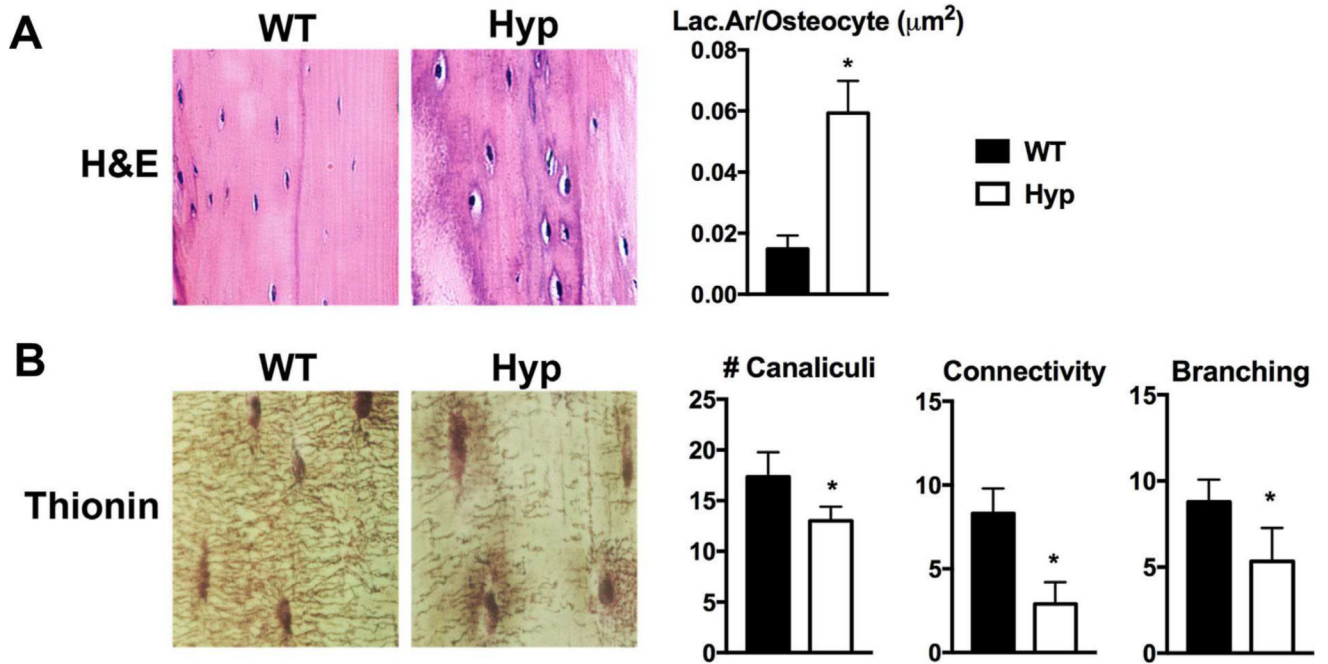
Fig. 1.
The cortical bones of Hyp mice exhibit abnormal osteocyte lacunar and canalicular morphology. (*A*) H&E stain of d75 WT and Hyp tibial cortices. Histomorphometric quantitation of Lac.Ar normalized to osteocyte number (Lac.Ar/osteocyte); measurements were made proximal and contralateral to the tibiofibular junction. (*B*) Thionin staining of the canalicular network in d75 WT and Hyp tibial cortices. Quantitation of number of canaliculi/osteocyte, canalicular connectivity, and canalicular branching. Data are representative of that obtained from 3 mice per genotype. *$p < 0.05$. Lac.Ar = lacunar area.
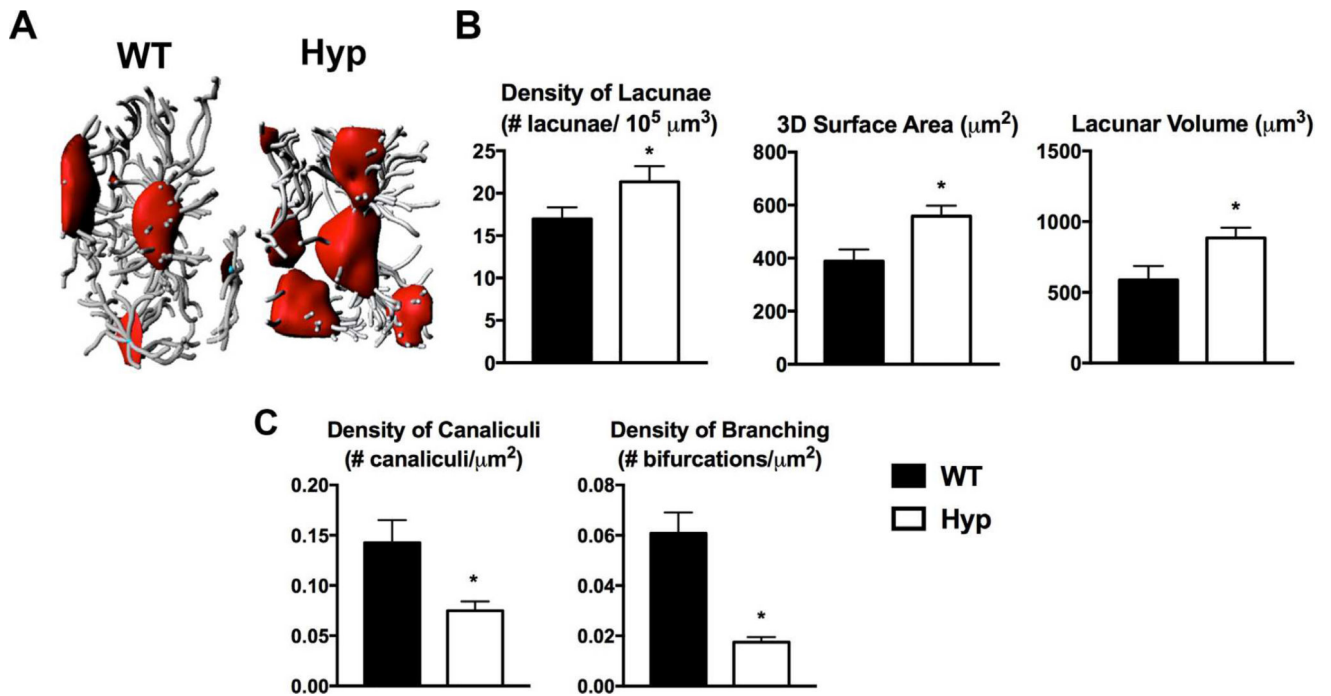
Fig. 2.
Intravital microscopy of WT and Hyp calvaria demonstrates increased 3D lacunar size and decreased density of canaliculi in Hyp mice. (**A**) THG microscopy performed on d30 WT and Hyp calvaria. Representative 3D renderings of the osteocyte lacunocanalicular network was created with Imaris software using the microscopic images. (*B*) Quantitation of lacunar density, volume, and 3D surface area. (*C*) Evaluation of density of canaliculi and density of branched canaliculi extending from lacunar surface. Data are representative of that obtained from 4 mice per genotype. *$p < 0.05$. THG = third harmonic generation.
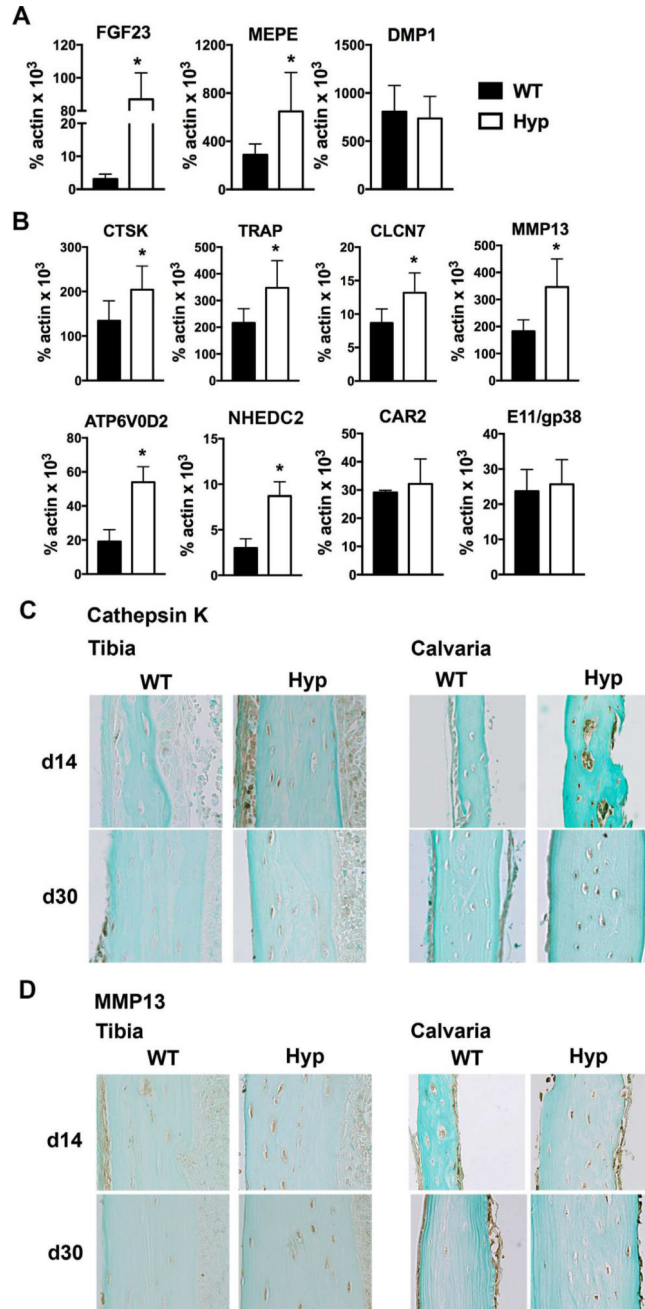
Fig. 3.

Hyp osteocytes have increased expression markers of perilacunar and canalicular remodeling. (*A*) RNA was isolated from osteocyte enriched WT and Hyp femoral cortices and subjected to RT-qPCR to quantitate mRNA expression of FGF23, MEPE, and DMP1. (*B*) mRNA expression of genes implicated in osteocyte perilacunar/canalicular remodeling. (*C*) Immunohistochemistry for cathepsin K on d14 and d30 tibia and calvaria. (*D*) Immunohistochemistry for MMP13 on d14 and d30 tibia and calvaria. Data are representative of that obtained from 3 mice per genotype/age. *$p < 0.05$.
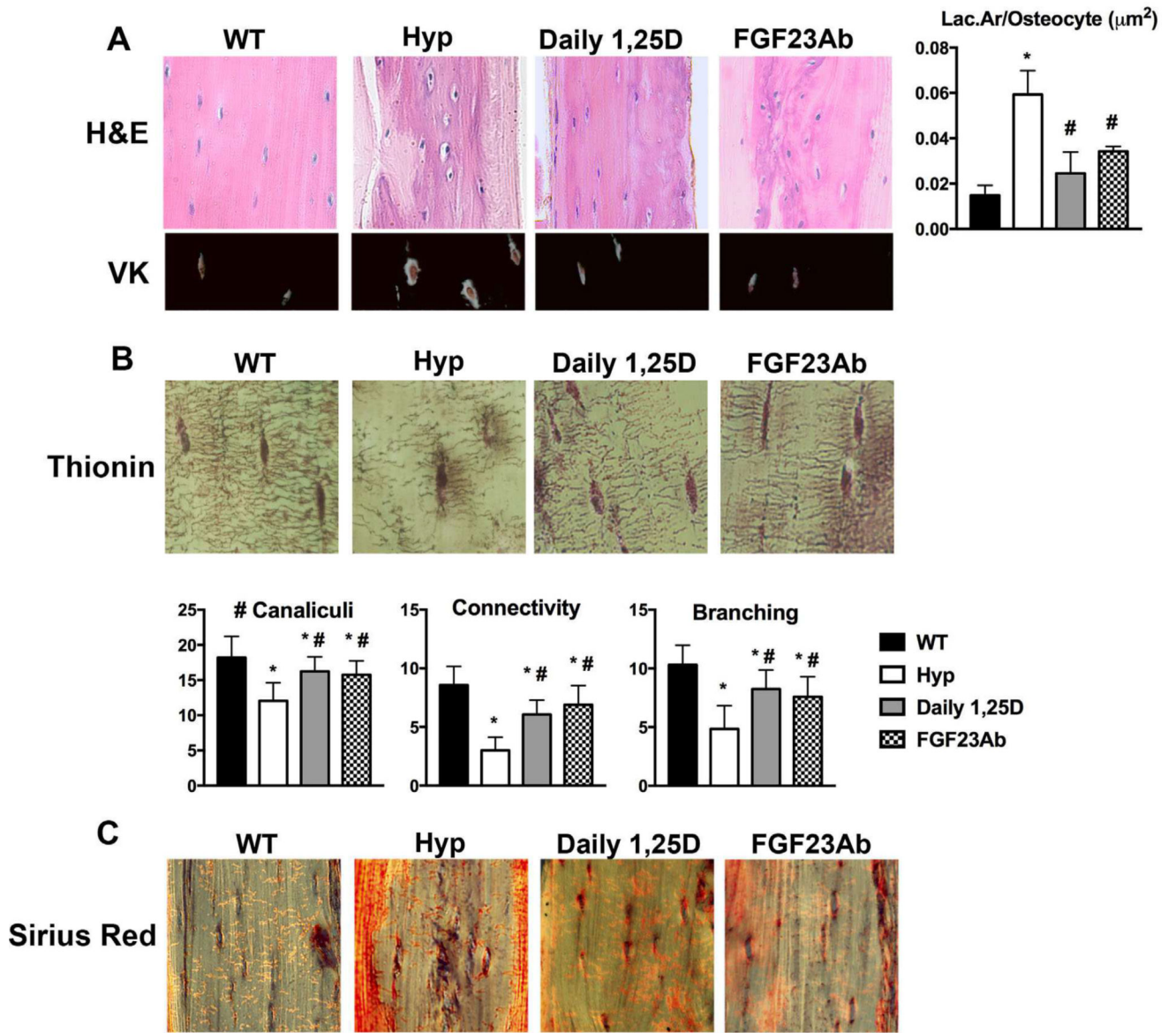
Fig. 4.
1,25D or FGF23Ab treatment normalizes tibial osteocyte lacunar area and improves canalicular organization in Hyp mice. (*A*) H&E and VK stain of d75 tibial cortices. Histomorphometric quantitation of Lac.Ar/osteocyte in d75 tibial cortical bone. (*B*) Thionin staining of canalicular network organization in d75 tibial cortices. Quantitation of canalicular number/osteocyte and canalicular connectivity and branching. (*C*) Picrosirius Red stain of d75 tibial cortices. Data are representative of that obtained from 3 mice per genotype. $*p < 0.05$, $\#p < 0.05$ versus Hyp. VK = von Kossa.
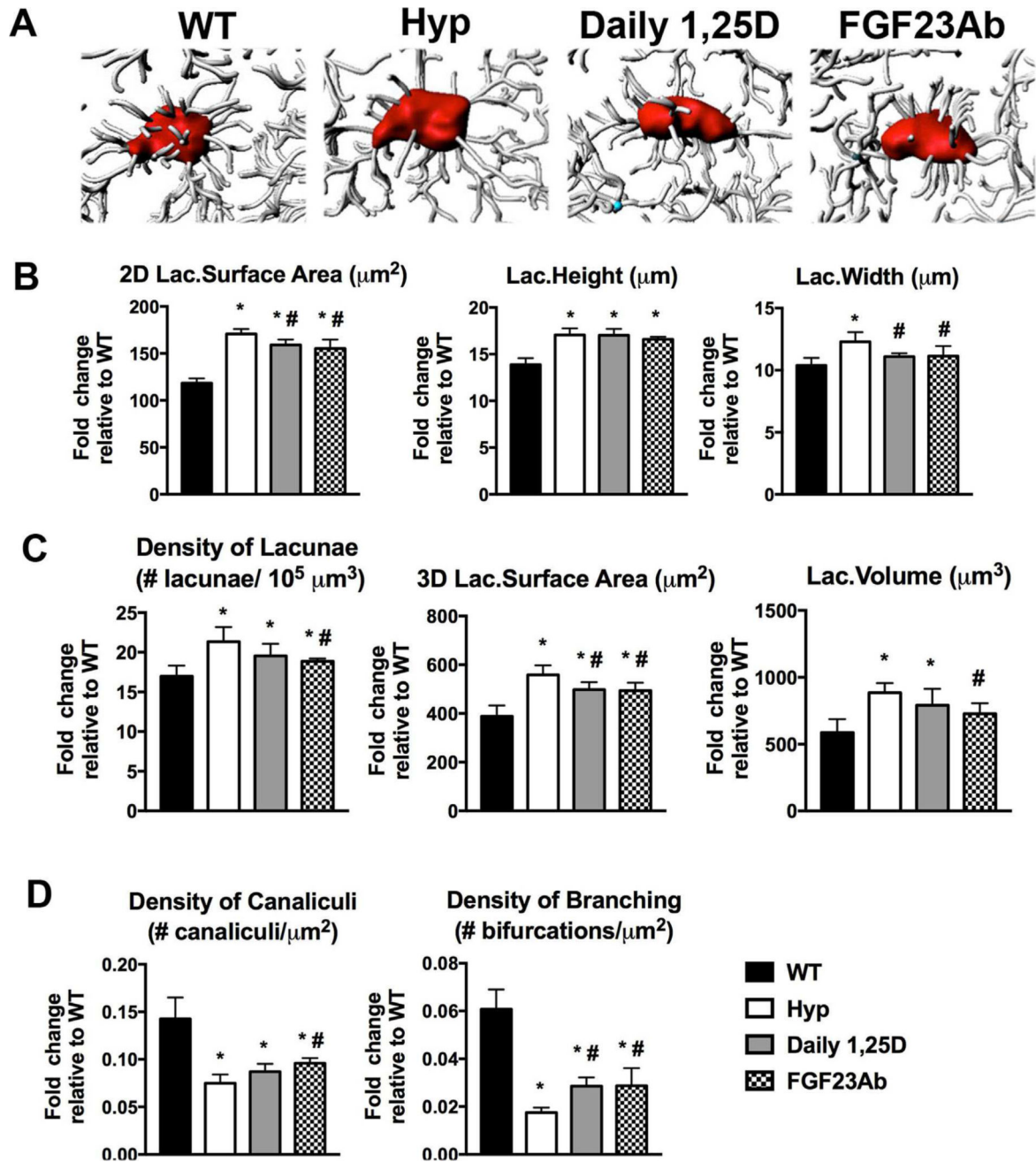
Fig. 5.
Treatment of Hyp mice with 1,25D or FGF23Ab partially restores calvarial lacunocanalicular network morphology. Intravital THG microscopy was performed on d30 mice. (*A*) Imaris software was used to produce 3D images of the osteocyte lacunae and canaliculi. (*B*) Evaluation of 2D lacunar (lac.) surface area, width, and height. (*C*) Quantitation of lacunar density, 3D surface area, and volume. (*D*) Quantitation of canalicular density and density of branched canaliculi extending from each lacuna. Data are representative of that obtained from 4 mice per genotype/treatment group. $*p < 0.05$, $\#p < 0.05$ versus Hyp.
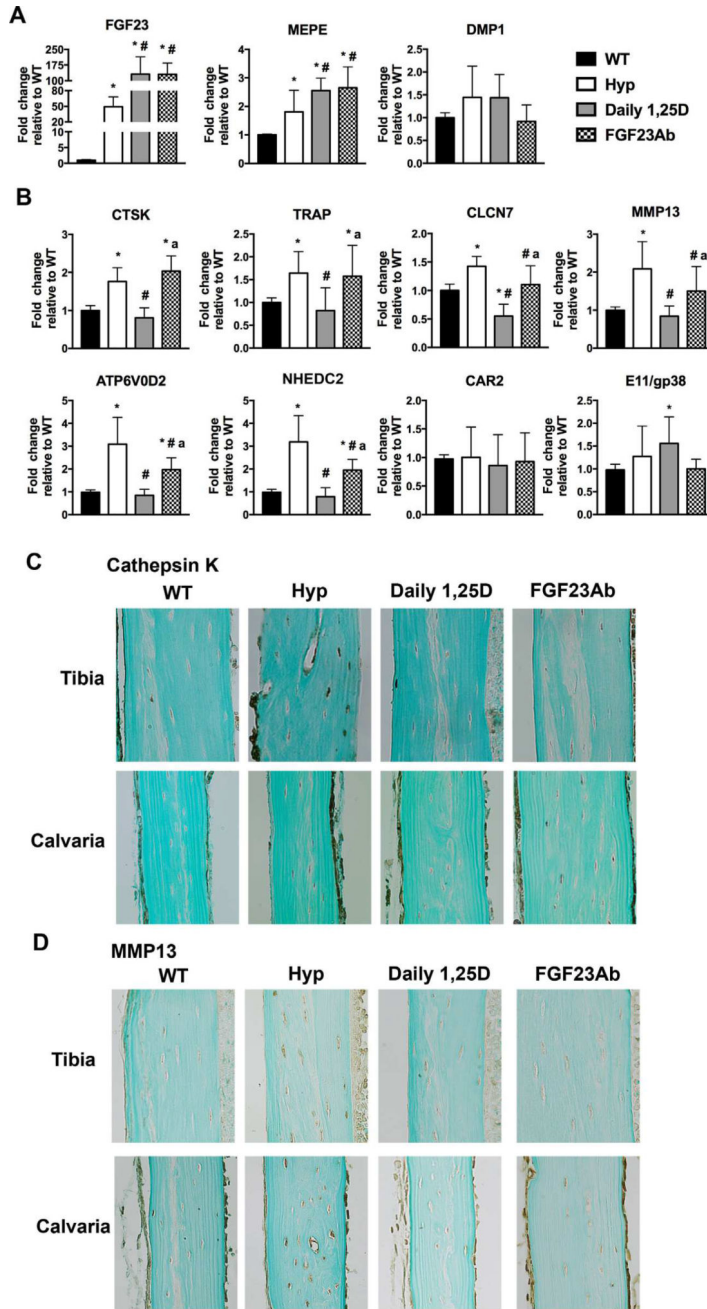
Fig. 6.

1,25D therapy restores expression of markers of perilacunar and canalicular remodeling in Hyp mice. mRNA and protein expression of markers of osteocyte lacunocanalicular remodeling was evaluated in d30 osteocyte-enriched femoral cortices. (*A*) FGF23, MEPE, and DMP1 mRNA expression. (*B*) mRNA expression of genes important for bone resorption and canalicular remodeling. (*C*) Immunohistochemical analysis of cathepsin K in d30 tibia and calvaria. (*D*) Immunohistochemistry for MMP13 in d30 tibia and calvaria. Data are

representative of that obtained from 5 mice per genotype/treatment group. *$p < 0.05$, #$p < 0.05$ versus Hyp, [a]$p < 0.05$ versus Daily 1,25D.